Lab on a Chip

Cite this: *Lab Chip*, 2012, **12**, 4748–4754

PAPER

Highly sensitive microscale *in vivo* sensor enabled by electrophoretic assembly of nanoparticles for multiple biomarker detection

Asanterabi Malima,[a] Salome Siavoshi,[a] Tiziana Musacchio,[b] Jaydev Upponi,[b] Cihan Yilmaz,[a] Sivasubramanian Somu,[a] William Hartner,[b] Vladimir Torchilin[b] and Ahmed Busnaina*[a]

Received 7th February 2012, Accepted 24th August 2012
DOI: 10.1039/c2lc40580f

This paper describes a microscale *in vivo* sensor platform device for the simultaneous detection of multiple biomarkers. We designed the polymer-based biosensors incorporating multiple active isolated areas, as small as 70 μm × 70 μm, for antigen detection. The fabrication approach involved conventional micro- and nano-fabrication processes followed by site-specific electrophoretic directed assembly of antibody-functionalized nanoparticles. To ensure precise and large-scale manufacturing of these biosensors, we developed a semi-automated system for the attachment of the 250-μm biosensor to a 300-μm catheter probe. Our fabrication and post-processing procedures should enable large-scale production of such biosensor devices at lower manufacturing cost. The principle of detection with these biosensors involved a simple fluorescence-based enzyme-linked immunosorbent assay. These biosensors exhibit high selectivity (ability to selectively detect multiple biomarkers of different diseases), specificity (ability to target generic to specific disease biomarkers), rapid antigen uptake, and low detection limits (for carcinoembryonic antigen, 31.25 pg mL^{-1}; for nucleosomes, 62.5 pg mL^{-1}), laying the foundation for potential early detection of various diseases.

Introduction

Biosensor discovery, which dates back to the 1960s, has its emphasis placed on the detection and monitoring of proteins, nucleic acids, and other biochemicals in medical applications.[1] Such biosensors are very valuable tools for diagnostics and regular therapeutic screenings of various diseases. They can be used not only to detect biological entities but also to monitor various developmental stages of particular diseases or biological processes. Recent advances in nanotechnology, materials, biology, and fluorescent spectroscopy have raised the potential for highly sensitive, multiple-marker detections of various diseases using a single device.[2–6] Nevertheless, current devices adapted for multiplex detection are either bulky or not biocompatible, making them unsuitable for implantation. These biosensors would be further improved through the addition of such features as remote testability, affordability, high reliability, ease of use, rapid screening, and the capability of early detection of diagnostic markers. The development of sensors with high sensitivity for the simultaneous *in vivo* detection of multiple biomarkers will be essential for the early diagnosis and treatment of diseases.

[a]*NSF NSEC Center for High-Rate Nanomanufacturing, Northeastern University, Boston, MA 02115, USA. E-mail: a.busnaina@neu.edu; Fax: +1 617 373 3266; Tel: +1 617 373 8297*
[b]*Center for Pharmaceutical Biotechnology and Nanomedicine, Northeastern University, Boston, MA 02115, USA*

Although commercially available biosensors based on antibody/antigen-based enzyme-linked immunosorbent assays (ELISAs)[7] have very high specificity, they lack the sensitivity necessary for the early detection of diseases, primarily because the randomness of the orientation and distribution of the antibodies on the sensor substrate result in a low number of antibody–antigen binding events.[8] Several recent efforts aimed at controlling the orientation and distribution of antibodies have employed uniformly distributed nanoparticles (NPs) coated with antibodies on a sensor substrate,[9–11] resulting in biosensors with improved sensitivity.

Temporary implant of these biosensors for *in vivo* disease monitoring with its large volume, whole blood screening capability may enhance the possibility of early disease detection. Recently, much emphasis has been directed towards *in vivo* sensors,[12] due to their improved reliability and sensitivity. For biosensors to be suitable for implantation, however, several issues, notably size and biocompatibility, must be addressed. In addition, biosensor probes for *in vivo* analysis must be sufficiently small for ready insertion into the bloodstream.

The preparation of many current biosensor devices takes full advantage of the materials and processing tools used for microfabrication. As a result, devices such as BioMEMS have been manufactured in large quantities at low unit cost.[13] For these *in vivo* devices to be effective, however, problems of biofouling must be overcome. Quantitative studies on biocompatibility and biofouling, conducted on device material selections for medical applications, as well as considerations of the

interactions of implantable devices within their biological environments, have suggested that Si-based MEMS, gold, and SU-8 devices are not only biocompatible, there are no cytotoxic materials when these devices where tested *in vivo* on mouse fibroblasts,[14] but also display minimized biofouling properties.[15,16]

In this study, our investigations into several biocompatible materials for device fabrication suggested that Si would be a good candidate because of its well-established micro- and nano-fabrication processes. For our biosensor design (Fig. 2a), however, the bulk fabrication of microscale Si devices would involve expensive and time-consuming processes such as deep reactive ion etching (DRIE) and laser machining for patterning. The high cost of these processes led us to choose SU-8 as a suitable candidate material for low-cost, bulk micro-fabrication of our devices. Therefore, we developed a process for fabricating an SU-8-based polymeric biosensor with potential applications for the *in vitro* and *in vivo* detection of multiple biomarkers. Our design for this microscale device allowed the assembly of arrays of multiple antibody-coated NPs on a single microchip surface, potentially enabling early diagnosis of several diseases using a single test probe. Utilizing a well-established NSF Center for High-Rate Nanomanufacturing (CHN)–directed assembly technique,[17] we selectively assembled NPs coated with specific antibodies onto a single microchip surface for the simultaneous detection of multiple biomarkers (Fig. 1). Antibodies attached as coatings on polymer nanospheres were selectively assembled into nanotrenches on the surface of the biosensor microchip. With well-oriented active antibody molecules acting as targets for blood-circulating biomarkers, the sensitivity of detection of the biosensor increased by up to five orders of magnitude[11] relative to that of the standard ELISA kit. Such highly sensitive biosensor devices should allow the early-stage detection of low concentrations of biomarkers of several diseases. Because the active region of our developed biosensor microchip is very small, attaching them onto the tip of a catheter required a micro-assembly manipulation system providing high dexterity, precise motion control, and visual feedback. To facilitate this assembly process, we employed a custom-built biosensor micro-assembly platform.[18]

In this study, we combined microfabrication and directed assembly techniques to fabricate a micro biosensor featuring arrays of NPs coated with specific antibodies directed against antigens overexpressed biomarkers including carcinoembryonic antigen (CEA), prostate specific antigen (PSA) and nucleosomes (NS). To develop the *in vivo* biosensors, we precisely attached the fabricated microscale sensors to catheters (see Fig. 1). The carboxylic functionalized nanoparticles interact with the Fc portion of the antibody *via* both ionic and hydrophobic interactions leading to the correct orientation of the antibodies on the surface modified nanoparticles (see Fig. 1). Immobilization of a monolayer of the antibodies onto NP surfaces by passive adsorption[19] also yields a uniform spatial distribution with decreased likelihood of non-specific binding in addition to the optimal antibody orientation.[20,21] The selective assembly of the functionalized NPs into nanotrench arrays on the surface of the microbiosensor enhances the spatial density distribution of the antibody-coated NPs. In addition, one of the major advantages of this biosensor is that detection of disease markers (potentially during routine physicals) could be performed *in vivo* without sample collection and storage.

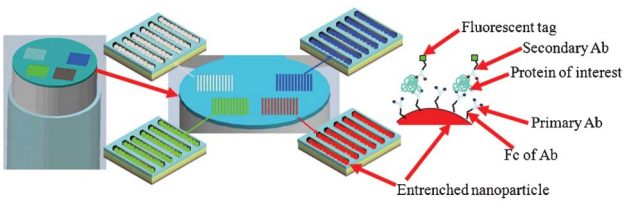

Fig. 1 Schematic representation of an *in vivo* biosensor featuring four areas assembled with antibody-coated NPs. The right-hand cartoon represents a sandwich ELISA platform for the detection of proteins.

Materials and methods

Design and fabrication of biosensor

We designed the biosensors in a circular structure that could be attached onto cylindrical microscale catheters (Fig. 2a). To do so, we positioned the biosensors onto a millimeter-scale holder that could be held by an end effector for precise alignment and manipulation.

Fabrication of the biosensor microchips was performed on 3-inch Si wafers (Fig. 2b), which served as microchip carriers during the microfabrication process. These wafers were cleaned with piranha solution (H_2SO_4:H_2O_2) for 5 min, rinsed with

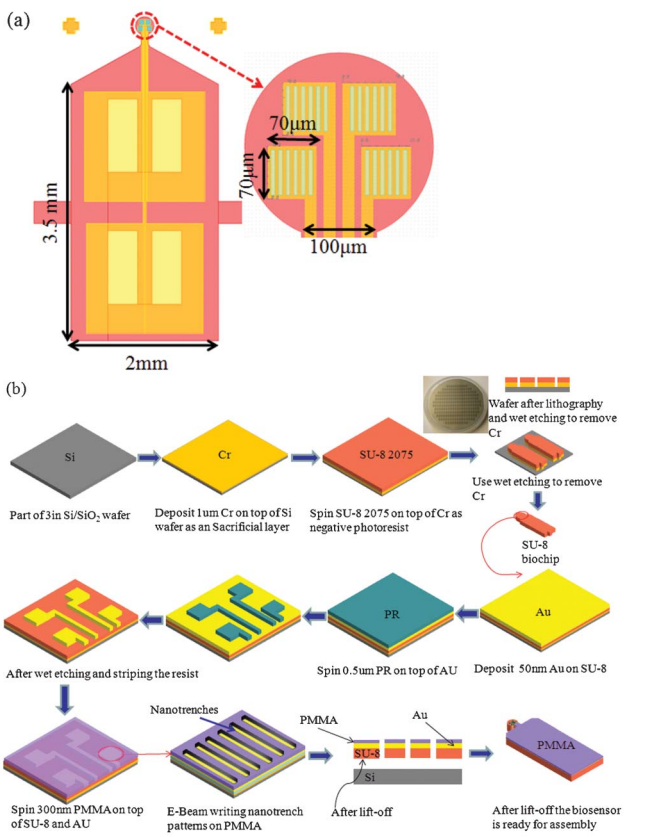

Fig. 2 (a) Design of the biosensor microchip: Holder with contact pads (left) and four separated biosensor regions (right) on a 250-μm-diameter biosensor. (b) Process schematic of the biosensor microchip's fabrication.

deionized water, and spun dry. A sacrificial layer of Cr (1 μm) was deposited using magnetron sputtering, ensuring that the biosensor microchips could be released after completing the microfabrication process. A 75-μm-thick SU-8 2075 negative tone photoresist was spun-coated onto the Cr/Si wafer. Pre- and post-exposure bakes were performed for 2 min at 65 °C followed by 8 min at 95 °C and for 2 min at 65 °C followed by 6 min at 95 °C, respectively. Exposure was performed for 34 s using a Quintel 4000-6 mask aligner operated at energy of 200 mJ cm^{-2}. Post-baking, the exposed patterns were developed in MicroChem SU-8 developer. After development, the exposed Cr was removed using a wet etch. The patterned SU-8 served as the substrate on which the biosensor was built.

To facilitate electrophoretic assembly of the NPs on the microchips, DC magnetron sputtering was used to deposit a 50-nm Au electrode layer on the SU-8 surface. The electrodes that were necessary to direct the various functionalized particles to their respective regions on the SU-8 were fabricated using the following procedure. A positive tone photoresist (PR) 1805 was spun on top of the Au layer and baked at 115 °C for 60 s. Exposure was performed for 4 s in the Quintel 4000-6 mask aligner, again at an energy of 200 mJ cm^{-2}. Development of the 1805 was performed for 45 s using Microchem MF 319 developer. The exposed Au was dry-etched in a Vecco Microetch Ion Mill for 4 min at an incident angle of 20°. The remaining 1805 mask was stripped in remover 1165 (1-methyl-2-pyrrolidinone) at 100 °C for 5 min.

To create the required nanotrenches that can hold and lock-in the nanoparticles on each of the four regions of the microscale Au patterns,[22] a 300-nm-thick Nano 950 PMMA layer was spun-coated, followed by baking at 100 °C for 120 s. E-beam lithography was then used to generate 500-nm-wide, 10-μm-long trench arrays with a pitch of 2.5–5 μm. The samples were then developed sequentially in a MIBK : IPA (1 : 3) mixture for 100 s, in IPA for 30 s, and in DI water for 5 min. The sacrificial layer of Cr was removed by placing the whole wafer in a Cr etchant for 1–2 h. After wet etching, the residual Cr etchant was removed by rinsing with DI water for 5 min. The design of a single biosensor microchip is displayed in Fig. 2(a); a schematic representation of the fabrication process is provided in Fig. 2(b).

Materials

Shipley 1805, SU-8 2075, and PMMA polymeric photoresist solutions and MIF 317 and MIBK developers were purchased from MicroChem (Newton, MA). Carboxyl-functionalized polystyrene beads (PSL-COOH, 5% w/v) were purchased from Sperotech (Lake Forest, IL). Nucleosome calf thymus antigen was purchased from Worthington Biochemical (Lakewood, NJ). Antinucleosome mAb 2C5 was obtained from Harlan Bioproducts (Indianapolis, IL), derived from a hybridoma cell line from our laboratory.[23] IgG-2a (Kappa) UPC 10 secondary antibody was purchased from MP Biochemicals (Solon, OH). Poly-L-lysine and bovine serum albumin were purchased from Sigma-Aldrich (St. Louis, MO). Oregon Green® 488 carboxylic acid succinimidyl ester-5-isomer was provided by Molecular Probes (Eugene, OR). BCA protein assay kits were purchased from Pierce Biotechnology (Rockford, IL). Mouse monoclonal antibody [1C7] to CEA, CEA protein, and secondary fluorescein-labeled goat polyclonal antibody to mouse IgG-H&L were obtained from Abcam (Cambridge, MA). All other chemicals and reagents were purchased in analytical grade from Sigma–Aldrich (St. Louis, MO).

Biosensor macro- and micro-assembly platform

Fig. 3(a) displays the platform configuration for biosensor macro- and micro-assembly. In this platform, the precision and accuracy of the assembly task relied on control performance and visual feedback. A central computer controlled the system components by using an object-oriented program. The developed software allowed all of the components of this platform to be controlled through a single modular program. For semi-automated macro-assembly tasks, a vision system was critical in providing reference for motion, depending on the extracted positional information from the encoders. Micro-assembly tasks were controlled by proper actuation of an active area of interest on the biosensor microchip surface.

Macro-assembly (attachment) of biosensor to catheter

The biosensor microchips (diameter: 250 μm) were aligned and attached to the tip of a 300-μm-diameter solid core nylon catheter using a high-precision control platform (shown in Fig. 3b). Assembly of the biosensor was conducted using a custom-built biosensor microassembly platform[18] featuring high-precision linear-encoded long travel stages (resolution: 100 nm) and charge-coupled device (CCD) cameras attached to objectives to provide visual feedback to a central computer. The schematic diagram, design metrics, and the operating procedure for this

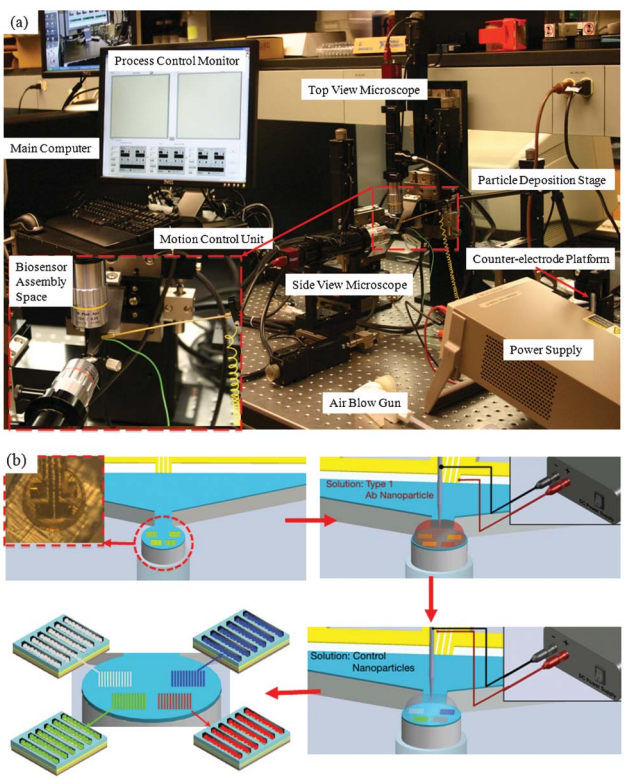

Fig. 3 (a) Biosensor macro- and micro-assembly platform picture. (b) Schematic representation of the NP micro-assembly tasks.

biosensor microassembly platform are discussed in detail elsewhere.[18] Assembly of an individual biosensor involved the following steps: (1) initialization of the system to the home position; (2) a fine 30G needle carrying a drop of highly viscous biocompatible glue was deposited at the end of the smoothly cut catheter; (3) a biosensor chip was placed onto the glue drop at the catheter tip; (4) after curing of the glue, antibody-coated NPs were selectively assembled into each of the isolated microscale regions containing the nano-scale trenches; (5) the biosensor microchip was separated from the holder through the action of a high-intensity laser beam. The assembled biosensors were stored in DI water prior to testing. Fig. 4 presents a schematic representation of the attachment process and the separation of the micro-biosensor active region from the holder.

Antibody functionalization of NPs

To improve the sensitivity of the biosensor, the biomarker receptors attached to the support required suitable orientations to ensure binding activity. A monolayer of antibody on the PSL NPs was deposited through passive adsorption. In this case, an excess amount of monoclonal antibody (mAb, 1.2 mg) required to saturate the nanoparticle surface was added to carboxyl polystyrene particles (1% w/v, 10 mg) in phosphate-buffered saline (PBS, pH 7.4, 1 mL). This mixture was incubated overnight at room temperature with constant stirring; it was then centrifuged (1.5×10^3 rpm, 10 min). The precipitate was re-suspended in DI water for further characterization and the supernatant analyzed for its protein content using a bicinchoninic acid (BCA) protein assay kit to determine the yield of antibody coated on the polystyrene particles. Further characterization of the assembled NPs included determination of their size and zeta potential. The activity of the immobilized antibody was determined using an ELISA kit; the NPs remained stable, in terms of their size, zeta potential, and activity, for over a month.

Assembly of antibody-coated NPs onto biosensor

The mAb-coated PSL NPs were diluted in DI water and then NH_4OH was added to increase the pH (to 10.8) and conductivity of the NP suspension. In the nanoparticle suspension used for directed assembly, the high pH used in our suspension does not lead to nanoparticle agglomeration on the microchip surface

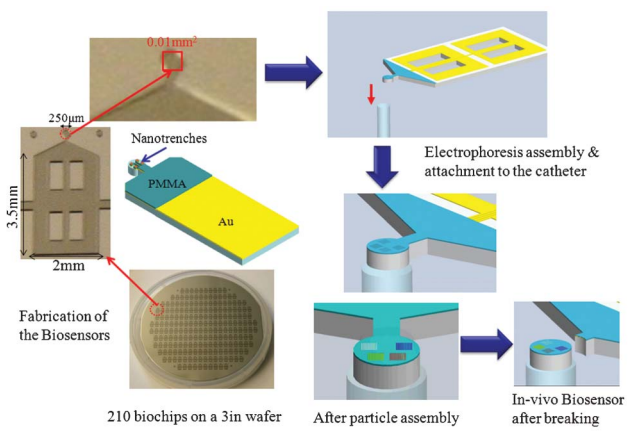

Fig. 4 Attachment of the biosensor to the catheter and separation of the biosensor microchip from the holder.

while low pH of suspension could result in agglomeration and insufficient assembly coverage in the trenches. Therefore, the suspension's pH and ionic conductivity were maintained at 10.8 and 450 μS, respectively, throughout the electrophoresis process. Because PSL NPs feature a stable negative zeta potential over a wide range of values of pH in aqueous solution,[24] the suspended NPs remained negatively charged.

A DC power supply was used to conduct the electrophoretic assembly onto the patterned PMMA/Au sensor as the anode and an Au counter electrode substrate as the cathode. A drop (20–30 μL) of the particle solution was placed onto the biosensor chip surface and then electrophoretic assembly of the NPs toward the nanotrenches was initiated. A picoammeter was used to monitor the current between the electrodes throughout the experiment. The electrostatic force acting on negatively charged colloidal NPs is directly proportional to the strength of the applied field and the charge on the NPs. The mAb-coated NPs were successfully assembled into the trenches when a voltage of 2.5 V was applied between the electrodes for 1–2 min. To keep the assembled NPs intact, the applied voltage was maintained while a washing buffer was used to remove the suspended solution from the microchip surface. This assembly process was repeated three times with other solutions containing different types of antibody-coated NPs. Finally, IgG-coated NPs (used as a control for detection) were assembled. The biosensor chips were stored in DI water to preserve the activity of their mAb-coated NPs until required for further testing. Before antigen detection, the biosensor microchips were blocked overnight with 2% bovine serum albumin (BSA) to reduce antigen non-specific binding on the PMMA surface.

Antigen assay and detection

The biosensor microchips were assembled with several types of antibody-coated NPs to detect different antigens under various environmental conditions. For the *ex vivo* trials, solutions (100 μL) with known concentrations of antigens in HEPES-buffered saline (HBS, pH 7.4) were injected into female mice *via* the tail vein. Blood was collected and assayed for CEA antigen using ELISA techniques. The antigen concentration in the mice was calculated by considering the total blood volume (*ca.* 2 mL) of mice as 8% of body weight. All experiments that involved the use of live animals were performed in compliance with the relevant laws and institutional guidelines. These experiments were approved by the Northeastern University Institutional Animal Care and Use Committee (IACUC). The biosensor microchips assembled with antibody-coated NPs were incubated with CEA antigen (in buffer or obtained from the blood of an animal previously spiked with a known concentration of CEA) for 2 h at 37 °C. For detection, the microchips were washed and then incubated with secondary FITC-labeled antibody for 2 h at room temperature. After washing, the chips were stored in PBS (pH 7.4) until they were required for fluorescence imaging using an optical fluorescence microscope. For NS detection, microchips assembled with mAb 2C5 coated nanoparticles were incubated with different concentrations of NS-labeled with an Oregon Green dye in fetal bovine serum (FBS). For control, the same antigen concentrations were simultaneously incubated on microchips assembled with IgG coated nanoparticles.

Results and discussion

Detection of antigens in blood, serum and buffer samples

We used blood *ex vivo* and a standard sandwich ELISA technique to investigate the activity of CEA on the biosensor and the efficacy of these biological devices. We imaged several biosensors presenting mAb CEA, mAb 2C5, mAb PSA and IgG antibodies and used Image J software to process and analyze their images. Fig. 5a reveals the strong fluorescence indicating the binding of secondary FITC-antibody to the CEA antigen at a concentration as low as 31.25 pg mL^{-1} in blood. Thus, the CEA antibodies on the NPs retained their activity and could identify CEA antigen in buffer and in blood. Our early results suggested sensitivity to concentrations of much less than 1 ng mL^{-1} (Fig. 5b)—a large increase in sensitivity relative to that of the commercially available ELISA detection kit.[25]

The microchips were also tested for NS using 2C5 antibody coated nanoparticles. In this case, tagged NS of concentration as low as 62.5 pg mL^{-1} in serum was detected (shown in Fig. 6). Also, Fig. 6a shows a comparison of the fluorescent signal after ELISA when mAb 2C5 and IgG functionalized nanoparticles were incubated with two different antigen concentrations of 500 pg ml^{-1} and 62.5 pg ml^{-1} of NS. Note that the fluorescence intensities of the mAb 2C5 were greater than that of the control

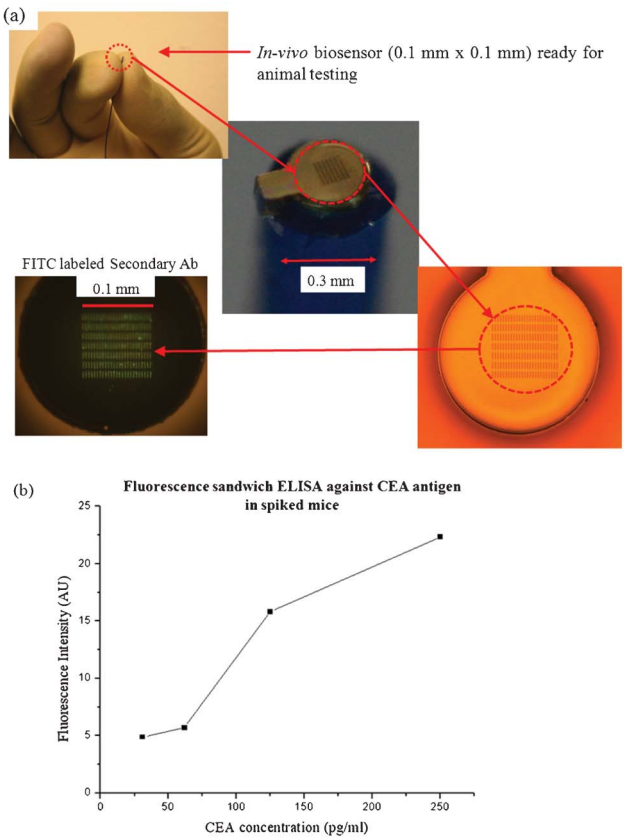

Fig. 5 (a) CEA detection in 50% murine blood after spiking with known concentrations in female Balb/C mice. (b) Fluorescence intensity obtained from image analysis of biosensor microchips treated with different concentrations of spiked antigens in 50% murine blood. The control for this test was the signal detected from the sample in the absence of antigens.

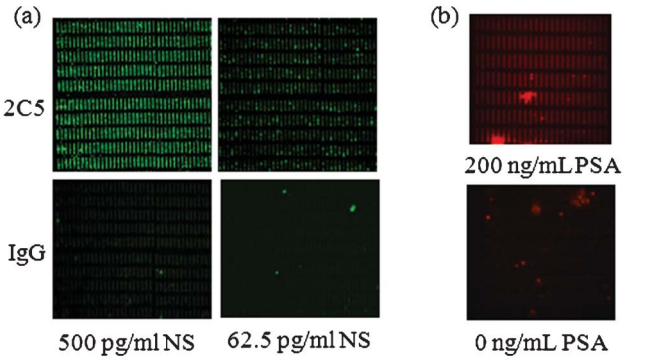

Fig. 6 (a) Fluorescence images revealing the presence of NS on 2C5-biosensor microchips. Images of mAb 2C5-NP assembled on the biosensors and incubated with different concentrations of Oregon Green®-labeled NS in serum, compared with those obtained at the same antigen concentrations on IgG-chips. (b) Images obtained after incubation with 200 ng mL^{-1} of PSA, and in its absence, in buffer.

IgG confirming the specificity of the mAb 2C5 detection toward NS (Fig. 6a). For PSA biomarker, microchips assembled with mAB PSA coated nanoparticles were incubated with different amounts of PSA in PBS buffer. The detection results in Fig. 6b exhibits different fluorescent signal levels for 200 ng ml^{-1} and 0 ng ml^{-1} of PSA after sandwich ELISA.

Selective assembly of nanoparticles on multiple-area microchip

The SU-8-based polymeric microscale biosensor was fabricated with multiple active and separate areas (each 70 μm × 70 μm). The electrically isolated areas enabled us to perform electrophoresis separately on each region of the microchip and, therefore, selective assembly of NPs coated with specific antibodies in well-defined nanotrenches for simultaneous multiplex detection. Prior to assembly of the antibody (2C5, CEA, and IgG)-coated NPs, the microchips exhibited good assembly coverage characteristics after assembling red fluorescent NPs on selected isolated areas of the biosensor (Fig. 7a); we then performed concentration dependent test experiments with varying amounts of CEA incubated with the microchips. Fig. 7b reveals the assembly of 320-nm CEA antibody-coated PSL and 100- and 60-nm red fluorescent PSL particles on three of the four regions of a microbiosensor; the fourth region, where electrophoresis was not performed, featured no assembled particles. Fig. 7c shows the detection of NS and cardiac myosin both at 500 ng ml^{-1} using mAb 2C5 and mAb 2G4 with mAb IgG as control; no cross-reaction between NS and cardiac myosin was observed.

This developed biosensor is very small (0.25 mm in diameter) and is attached to a catheter (0.3 mm in diameter) such that it can be temporary implanted into a vein for 5–10 min for large volume, whole blood screening without biofouling. Our experiments show that the biosensor has small traces of biofouling after 30 min and significant biofouling after incubation for more than 2 h in whole blood. This biosensor has potential advantages compared to traditional *in vitro* techniques because it enables disease markers detection with less false positives with a very low detection limit. This capability will be very useful for detecting very small changes in biomarker concentration in disease monitoring.

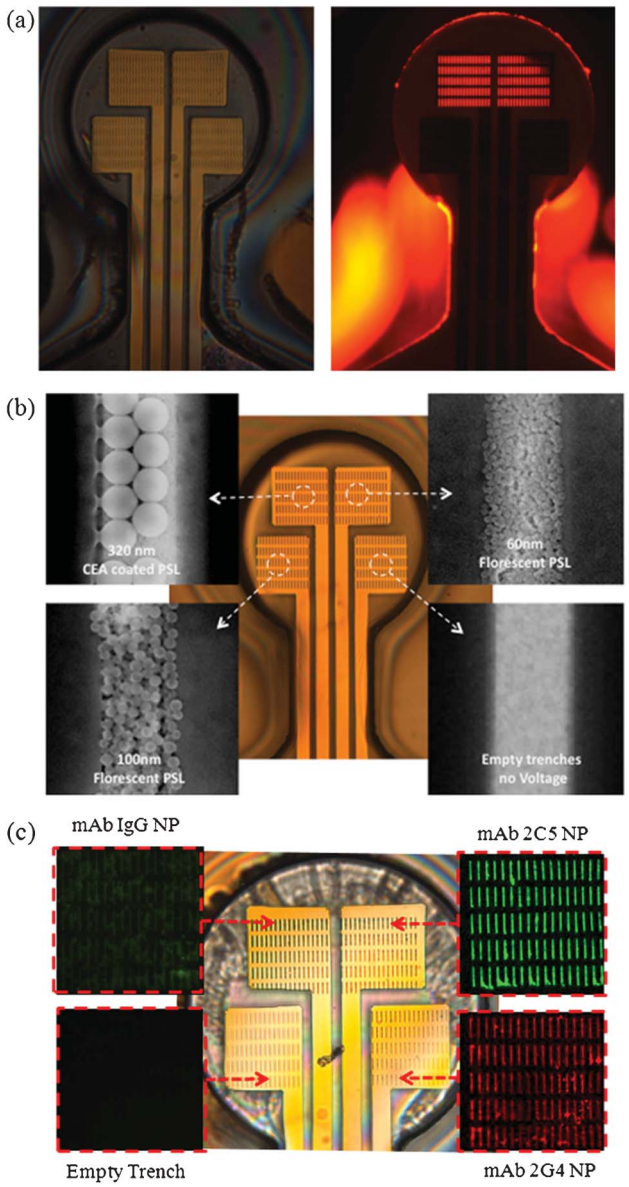

Fig. 7 (a) Bright field image (left) and dark field image (right) for red fluorescent PSL NPs assembled on two selected area of the biosensor. (b) Optical and SEM images of a biosensor with four electrically separated regions in which electrophoretic assembly was performed individually to assemble various NPs. (c) Detection of NS and myosin at 500 ng mL^{-1} using 2C5 and mAb 2G4 with mAb IgG as control.

Challenges

The biosensor fabrication process described here is relatively simple compared to currently used multi-level masks semiconductor techniques. One of the challenges when generating multiple regions on a single microchip active area is aligning the multi-level masks (if optical lithography is used). As shown in Fig. 7, the biosensor device neck (length: 100 μm) incorporated conducting line features placed 10 μm apart, a distance close to optical lithographic limitations. Therefore, we performed several experiments, varying the thickness of the second-level photoresist mask alignment parameters to ensure optimal isolated electrode structures (when using optical lithography).

Also, the electrophoretic assembly of the NPs was governed by several parameters, including the applied voltage, assembly time, particle concentration, and surface charge. Among these parameters, the particle charge would vary from particle to particle, depending on their types and dimensions. In addition, depending on their functionalization, NPs can present different surface charges, which are greatly influenced by the solution properties (*e.g.*, ionic strength, pH).[26] Therefore, the particle charge would not be exactly the same for each type of antibody-coated NP, potentially varying the nature of the NP assembly process. In such a case, optimizing the assembly parameters for each type of NP would be advisable to achieve complete NP coverage in the trenches.

Future considerations

Similar to the ELISA based measurements, standards must be developed to quantify unknown concentrations of experimental and clinical samples.[27] Therefore, additional experiments must be conducted on this multiple-marker biosensor platform to develop the standard curve that can be used for absolute quantification to determine the values of unknown antigen concentrations. Alternatively, to realize a biosensor device having the ability to simultaneously detect multiple antigens (more than two antigens simultaneously) at very low concentrations, a relative quantification method can also be used. To do this, an additional biochip specifically developed for testing control standards could be used as reference in parallel with multiple biomarker detection. These approaches would provide the ability to quantify the values of up to four biomarkers in tested samples.

Conclusions

We have developed a microscale *in vivo* biosensor device platform having the potential to simultaneously detect multiple biomarkers. We used standard fabrication techniques to develop *in vivo* biosensor microchips featuring four separate areas for the assembly of four different types of biomarker-coated NPs. We prepared biocompatible polymer-based microchips using an SU-8 template, not only to minimize the fabrication cost but also to simplify the attachment of the sensors to catheter probes and their separation from the holder following NP assembly. A wide range of antigens could potentially be analyzed using such a platform. Herein, we report a microscale sensing device with increased sensitivity for the detection of CEA relative to that of commercial ELISA detection assay kits.

In this study, we limited our coatings for the NPs to readily available specific biomarkers, as a test of our ability to develop a multiple-biomarker sensing device. Such a device's use could be extended to investigate a wide range of biomarkers applied to different nanoelements (*e.g.*, nanowires, assembled nanotubes), monitoring not only through fluorescence-based ELISAs on coated NPs but also through conductance measurements on biomarker-coated nanowires and nanotubes.

Integrating the developed biosensor with miniaturized fluorescence spectrophotometer and readouts[28,29]can lead to portable Lab on a Chip (LOC) systems for simultaneous multiple disease diagnostic and screening applications in remote areas drastically reducing health care cost and saving lives. Moreover the possibility

of having electrical output signal rather than an optical signal would result in reduction of LOC system footprint leading to a portable LOC system for detection of biomarkers.

Acknowledgements

This study was supported by the W. M. Keck Foundation (grant no. 06-003599A00) and the National Science Foundation Nanoscale Science and Engineering Center for High-Rate Nanomanufacturing (grant no. 0832785). Experiments were conducted at the George J. Kostas Nanoscale Technology and Manufacturing Research Center at Northeastern University with collaborators from the Center for Pharmaceutical Biotechnology and Nanomedicine.

References

1 G. S. Wilson and R. Gifford, Biosensors for real-time in vivo measurements, *Biosens. Bioelectron.*, 2005, **20**, 2388–2403.
2 E. Stern, A. Vacic, N. K. Rajan, J. M. Criscione, J. Park, B. R. Ilic, D. J. Mooney, M. A. Reed and T. M. Fahmy, Label-free biomarker detection from whole blood, *Nat. Nanotechnol.*, 2010, **5**, 138–142.
3 Y. Choi, J. Kwak and J. W. Park, Nanotechnology for early cancer detection, *Sensors*, 2010, **10**, 428–455.
4 G. Zheng, F. Patolsky, Y. Cui, W. U. Wang and C. M Lieber, Multiplexed electrical detection of cancer markers with nanowire sensor arrays, *Nat. Biotechnol.*, 2005, **23**, 1294–1301.
5 L. Ma, Y. Hong, Z. Ma, C. Kaittanis, J. M. Perez and M. Su, Multiplexed highly sensitive detections of cancer biomarkers in thermal space using encapsulated phase change nanoparticles, *Appl. Phys. Lett.*, 2009, **95**, 043701.
6 K. D. Barbee, A. P. Hsiao, E. E. Roller and X. Huang, Multiplexed protein detection using antibody-conjugated microbead arrays in a microfabricated electrophoretic device, *Lab Chip*, 2010, **10**, 3084–3093.
7 E. Engvall and P. O. Perlmann, *Immunochemistry*, 1971, **8**, 871–875.
8 M. J. Taussig and U. Landegren, Progress in antibody arrays, *Targets*, 2003, **2**(4), 169–176.
9 J. Nam, C. S. Thaxton and C. Mirkin, Nanoparticles-based bio-bar codes for the ultrasensitive detection of proteins, *Science*, 2003, **301**, 1884–1886.
10 X. Luo, A. Morrin, A. Killard and M. R. Smyth, Application of nanoparticles in electrochemical sensors and biosensors, *Electroanalysis*, 2006, **18**, 319–326.
11 K. L. Brogan, K. N. Wolfe, P. A. Jones and M. H. Schoenfisch, Direct oriented immobilization of F(ab') antibody fragments on gold, *Anal. Chim. Acta*, 2003, **496**, 73–80.
12 J. Wang, Electrochemical glucose biosensor, *Chem. Rev.*, 2008, **108**, 814–825.
13 V. Vickerman, J. Blundo, S. Chung and R. D. Kamm, Design, fabrication and implementation of a novel multi parameter control microfluidic platform for three-dimensional cell culture and real-time imaging, *Lab Chip*, 2008, **8**, 1468–1477.
14 G. Kotzar, M. Freas, P. Abel, A. Fleischman, S. Roy, C. Zorman, J. M. Moran and J. Melza, Evaluation of MEMS materials of construction for implantable medical devices, *Biomaterials*, 2002, **23**, 2737–2750.
15 G. Voskerician, M. S. Shive, R. S. Shawgo, H. von Recum, J. M. Anderson, M. J. Cima and R. Langer, Biocompatibilty and biofouling of MEMS drug delivery devices, *Biomaterials*, 2003, **24**, 1959–1967.
16 P. M. George, A. W. Lyckman, D. A. LaVan, A. Hedge, Y. Leung, R. Avasare, C. Tesla, P. M. Alexander, R. Langer and M. Sur, Fabrication and biocompatibility of polypyrrole implants suitable for neural prosthetics, *Biomaterials*, 2005, **26**, 3511–3519.
17 X. Xiong, P. Makaram, A. Busnaina, K. Bakhtari, S. Somu, N. McGruer and J. Park, *Appl. Phys. Lett.*, 2006, **89**, 193108.
18 A. Malima, A. Busnaina and S. Somu, Biosensor microassembly platform: Design and automation, *Proceedings of ASME (IDETC/CIE2009)*, 2009, 485–489.
19 L. A. Cantarero, J. E. Butler and J. W. Osborne, The adsorptive characteristics of proteins for polystyrene and their significance in solid-phase immunoassays, *Anal. Biochem.*, 1980, **105**, 375–382.
20 I. Vikholm and W. M. Albers, Oriented immobilization of antibodies for immunosensing, *Langmuir*, 1998, **14**, 3865–3872.
21 S. Babacan, P. Pivarnik, S. Letcher and A. G. Rand, Evaluation of antibody immobilization methods for piezoelectric biosensor application, *Biosens. Bioelectron.*, 2000, **15**, 615–621.
22 S. Siavoshi, C. Yilmaz, S. Somu, T. Musacchio, J. Upponi, V. Torchilin and A. Busnaina, Size-selective template-assisted electrophoretic assembly of nanoparticles for biosensing applications, *Langmuir*, 2011, **27**, 7301–7306.
23 L. Z. Iakoubov and V.P. Torchilin, A novel class of antitumor antibodies: nucleosome-restricted antinuclear autoantibodies (ANA) from healthy aged nonautoimmune mice, *Oncol. Res.*, 1997, **9**, 439–446.
24 H. Lin, *Ph.D. dissertation*, Clarkson University, Potsdam, New York, 2001.
25 W. Dungchai, W. Siangproh, J. M. Lin, O. Chailapakul, S. Lin and X. Ying, Development of a sensitive micro-magnetic chemiluminescence enzyme immunoassay for the determination of carcinoembryonic antigen, *Anal. Bioanal. Chem.*, 2007, **387**, 1965–1971.
26 D. F. Evans and H. Wennerström, *The Colloidal Domain: Where Physics, Chemistry, and Biology Meet*. 1999, Wiley-VCH, New York.
27 H. Buss, T. P. Chan, K. B. Sluis, N. M. Domigan and C. C. Winterbourn, Protein carbonyl measurement by a sensitive ELISA method, *Free Radical Biol. Med.*, 1997, **23**, 361–366.
28 M. Yao, G. Shah and J. Fang, Highly sensitive and miniaturized fluorescence detection system with an autonomous capillary fluid manipulation chip, *Micromachines*, 2012, **3**, 462–479.
29 R. Walczak, Fluorescence detection by miniaturized instrumentation based on non-cooled CCD minicamera and dedicated for lab-on-a-chip applications, *BioChip J.*, 2011, **5**, 271–279.

